Research Square

Preprints are preliminary reports that have not undergone peer review.
They should not be considered conclusive, used to inform clinical practice,
or referenced by the media as validated information.

Stress-induced ClpP drives metabolic rewiring and adaptation to microenvironmental stress in cancer cell

Sophie Curbo
Karolinska Institutet
Janne Purhonen
Karolinska Institutet
Feifei Feng
Zhengzhou University
Wei Wang
Zhengzhou University
Xiaoshan Zhou
xiaoshan.zhou@ki.se
Karolinska Institutet

Research Article

Keywords: ClpP, cancer metabolism, hypoxia, metabolic adaptation, tumor microenvironment

Posted Date: November 12th, 2026

DOI: https://doi.org/10.21203/rs.3.rs-11061932/v1

License: This work is licensed under a Creative Commons Attribution 4.0 International License.
Read Full License

Additional Declarations: No competing interests reported.

Abstract

Background

The mitochondrial protease ClpP is frequently upregulated in multiple cancer types and has emerged as a promising therapeutic target. However, the regulation of ClpP expression under cellular stress and the biological consequences of elevated ClpP levels remain incompletely understood. We investigated how metabolic, environmental, and therapeutic stressors influence ClpP expression and examined the impact of elevated ClpP expression on cancer cell adaptation to adverse microenvironmental conditions.

Methods

ClpP expression was assessed in cancer cell lines exposed to nutrient deprivation, hypoxia, and pharmacological stressors. Stable ClpP-overexpressing cell lines were established to evaluate the effects of elevated ClpP expression on cell survival, mitochondrial respiratory enzyme activities, redox status, ATP levels, extracellular acidification, and expression of genes involved in metabolic adaptation.

Results

ClpP expression was dynamically regulated by cellular stress. Cisplatin, LY294002, and 2-deoxyglucose increased ClpP expression, whereas metformin, ONC201, and hypoxia reduced ClpP levels. ClpP overexpression enhanced cell survival under nutrient-deprived and hypoxic conditions. Elevated ClpP expression was associated with reduced mitochondrial respiratory enzyme activities, decreased NAD+/NADH ratios, and maintenance of intracellular ATP levels. In addition, ClpP-overexpressing cells exhibited reduced extracellular acidification during prolonged culture and increased expression of mitochondrial carbonic anhydrase 5B (CA5B) together with genes involved in the serine-one-carbon-folate pathway and uridine metabolism.

Conclusions

ClpP is a stress-responsive mitochondrial factor whose elevated expression is associated with enhanced survival under nutrient and oxygen limitation. These effects are accompanied by coordinated changes in bicarbonate homeostasis, one-carbon metabolism, and uridine utilization, suggesting a potential role for ClpP in metabolic adaptation to adverse tumor microenvironmental conditions.

Background

ClpP is a critical component of the mitochondrial proteostasis machinery. Together with the ATP-dependent unfoldase ClpX, ClpP forms the ClpXP complex, which selectively degrades misfolded or damaged proteins and thereby preserves mitochondrial protein homeostasis [1–3]. Accumulating

evidence indicates that ClpP is frequently upregulated across multiple cancer types [4–7], and elevated expression has been associated with tumor progression and poor prognosis [6, 8, 9]. Intriguingly, both inhibition and hyperactivation of ClpP can induce selective cancer cell death, underscoring the complex role of ClpP in tumor biology and its potential as a therapeutic target [4, 10, 11]. Accordingly, ClpP activators such as ONC201 and ONC212 are currently being evaluated in clinical and preclinical studies [12–15]

Basal ClpP expression level appears to be an important determinant of the anticancer efficacy of ClpP agonists [16–19]. However, the mechanisms that regulate ClpP expression remain poorly understood. It is unclear whether microenvironmental and therapeutic stressors, such as nutrient deprivation, hypoxia, anticancer drugs, modulate ClpP expression, and thereby influence cellular adaptation and treatment response. Currently, the anticancer effects of ClpP-targeting agents have been attributed to disruption of mitochondrial oxidative phosphorylation (OXPHOS), resulting in impaired ATP production and mitochondrial dysfunction. Nevertheless, emerging evidence suggests that the role of ClpP extends beyond the maintenance of mitochondrial bioenergetics. Perini, T. *et al* [7] reported that ClpP silencing does not significantly affect oxygen consumption or ATP levels in multiple myeloma cells, but instead alters anabolic pathways, including polyamine synthesis. Moreover, genetic disruption of ClpP promotes browning of white adipose tissue, further supporting a broader role for ClpP in metabolic regulation [20]. Together, these observations suggest that ClpP regulates metabolism beyond its established role in OXPHOS. Although ClpP is increasingly recognized as a therapeutic target, little is known about how elevated ClpP expression contributes to cancer cell fitness and survival within hostile tumor microenvironments

Tumor cells are continuously exposed to nutrient limitation, hypoxia and extracellular acidification. Adaptation to these conditions requires extensive metabolic remodeling. Whether elevated ClpP contributes to this adaptive response remains unknown. Here we tested the hypothesis that stress-induced ClpP contributes to metabolic adaptation that improves cancer cell survival under nutrient and oxygen limitation. We demonstrate that ClpP is dynamically regulated by distinct stressors and that elevated ClpP expression is associated with enhanced survival under metabolically challenging conditions and coordinated changes in bicarbonate metabolism, serine-one-carbon metabolism and uridine utilization pathways.

Results

1. Stress regulates ClpP expression

To determine whether ClpP is influenced by cellular stress, we first examined ClpP protein levels in three cancer cell lines (143B, A549, and HepG2) and a non-cancerous human lung fibroblast cell line (LF) during prolonged culture without medium replacement, a condition associated with progressive nutrient depletion and extracellular acidification. Under these conditions, ClpP levels gradually increased over time in all cell lines examined (Fig. 1A). To further investigate the regulation of ClpP by specific stress

stimuli, A549 cells were exposed to metabolic and genotoxic stressors. 2-deoxyglucose (2-DG), LY294002, and cisplatin all increased ClpP protein expression (Fig. 1B). We next tested how ClpP expression responds to metformin treatment because metformin enhances glycolysis and extracellular acidification in cancer cell lines [21–23]. We found that metformin treatment accelerated extracellular acidification in A549 cells (Supplementary Fig. 1A). Interestingly, metformin suppressed ClpP expression in the three tested cancer cell lines in a dose-dependent manner (Fig. 1C and 1D). We observed that ONC201, the first-in-class ClpP activator [24], also decreased ClpP protein levels in these cell lines (Fig. 1C and 1D). Additionally, hypoxic growth condition (1% O_2) also significantly decreased ClpP protein levels in A549 cells (Fig. 1E). Moreover, hypoxia largely abolished the induction of ClpP elicited by 2-DG and cisplatin (Fig. 1E). Collectively, these findings demonstrate that ClpP is regulated in a stress-specific manner, with different stressors inducing opposite effects on protein abundance.

2. ClpP overexpression impairs respiratory enzyme activities and alters NAD^+/NADH homeostasis without affecting ATP levels

To assess the functional consequences of elevated ClpP expression, we established cell lines stably expressing a ClpP-EGFP fusion protein (Supplementary Fig. 2A-2C). The ClpP-EGFP overexpressing cells exhibited extremely high sensitivity to ONC201 (Supplementary Fig. 2D and Supplementary table 1). However, ClpP overexpression did not affect cell proliferation under standard culture conditions in either cell line (Supplementary Fig. 2E and 2F). We next analyzed the effects of ClpP overexpression on activities of mitochondrial respiratory enzymes in 143B cells. All assessed enzymes showed a similar pattern of decreased activity in ClpP overexpressing 143B cells (143B-ClpP) compared to control cells 143B-EGFP, only expressing EGFP (Fig. 2A-D). Consistent with impaired mitochondrial oxidative metabolism, ClpP overexpression decreased the cellular NAD^+/NADH ratio without affecting total NAD(H) (Fig. 2E-2H). Surprisingly, despite the widespread reduction in respiratory enzyme activities and the altered redox balance, intracellular ATP levels remained unchanged (Fig. 2I), suggesting the engagement of compensatory metabolic pathways. To explore whether enhanced glycolysis acts as compensation, we assessed cellular sensitivity to the glycolytic inhibitor 2-DG. 143B-ClpP cells displayed only slightly increased sensitivity to 2-DG compared with control cells (Fig. 2J). Together, these findings demonstrate that elevated ClpP expression suppresses mitochondrial respiratory enzyme activity and perturbs cellular redox balance while maintaining ATP homeostasis, suggesting metabolic adaptation to compromised mitochondrial function.

3. ClpP overexpression is associated with increased survival under prolonged culture and hypoxic conditions

During prolonged culture, we observed that medium of A549 cells only expressing EGFP (A549-EGFP) became progressively more acidic from day 3 onwards, whereas the medium of ClpP-EGFP-expressing A549 cells (A549-ClpP) maintained a relatively stable pH (Fig. 3A). A similar, although less pronounced, trend was also observed in 143B cells (Fig. 3B). To investigate whether these differences were associated with altered extracellular lactate levels, we measured lactate concentrations in the culture

medium. Interestingly, lactate levels were comparable between 143B-ClpP cells and their corresponding control cells after 3 days of culture (Fig. 3C). In contrast, A549-ClpP cells exhibited significantly higher lactate levels than A549-EGFP cells on day 3 after seeding; however, this difference was no longer evident by day 6 (Fig. 3D). Notably, A549-ClpP and A549-EGFP cells displayed similar proliferation rates during the first 5 days of culture. Thereafter, A549-ClpP cells continued to proliferate and remained viable for up to 16 days without medium replacement. In contrast, A549-EGFP cells exhibited a marked reduction in proliferation after day 5 and lost viability after day 8 under the same conditions (Fig. 3E and 3F).

(A, B) Representative images showing culture medium color changes in A549 (A) and 143B (B) cells after 4 days of culture. (C) Lactate concentrations in conditioned medium collected from 143B cell lines on 3 days of culture. (D) Lactate concentrations in conditioned medium collected from A549 cell lines at the indicated time points following seeding. (E) Growth curves of A549-ClpP and A549-EGFP cells cultured under normoxic conditions without medium replacement. Data are presented as mean cell number ± SD from triplicate wells of a 24-well plate. (F) Representative images of A549-ClpP and A549-EGFP cells after 10 days of culture without medium replacement. Data are presented as mean ± SD. Statistical significance was determined using a two-tailed Student's t-test or one-way ANOVA test. *: $P < 0.05$; **: $P < 0.01$.

Moreover, A549-ClpP cells displayed substantially higher proliferation rates and survival than control cells when cultured under hypoxic conditions (1% O_2) (Fig. 4A and 4B), despite marked acidification of culture medium (Supplementary Fig. 1B). To further evaluate whether extracellular acidification contributes to the reduced survival of control cells, we increased the buffering capacity of the culture medium. Enhanced buffering significantly improved the viability of A549-EGFP cell in a dose-dependent manner after 10 days of culture under normoxic conditions, whereas no additional proliferation or survival benefit was observed in A549-ClpP cells (Fig. 4C). Together, these findings suggest that ClpP overexpression enhances survival under prolonged culture and hypoxic conditions, at least in part by protecting cells from the detrimental effects of extracellular acidification.

1. (A) Growth curves of A549-ClpP and A549-EGFP cells under hypoxic conditions (1% O_2) without medium replacement. Data are presented as mean cell number ± SD from triplicate wells of a 24-well plate. (B) Representative images of A549-ClpP and A549-EGFP cells cultured under hypoxic conditions. A549-EGFP cells underwent a pronounced morphological transition from a cobblestone-like epithelial phenotype to an elongated, spindle-shaped morphology. In contrast, A549-ClpP cells largely retained their epithelial morphology and reached confluency. (C) Effect of enhanced medium buffering on the viability of A549-ClpP and A549-EGFP cells cultured under normoxic conditions. Cells were cultured in medium supplemented with the indicated concentrations of HEPES. Data are represented as mean ± SD of three independent experiments. Statistical significance was determined by student t test or one-way ANOVA. *:$P < 0.05$; *** $P < 0.001$.

1. **4. Elevated ClpP expression accompanies changes in bicarbonate and serine-one-carbon-folate metabolism**

To investigate the metabolic adaptations associated with the enhanced survival of ClpP-overexpressing cells under nutrient deprivation and acidic microenvironmental conditions, we examined the expression of genes involved in lactate metabolism, bicarbonate homeostasis, and alternative nutrient utilization. Consistent with elevated extracellular lactate levels (Fig. 3D), A549-ClpP cells exhibited increased expression of genes associated with lactate production and transport (Fig. 5A). Given the increased acid burden associated with lactate accumulation, we next examined genes involved in bicarbonate homeostasis. Mitochondrial carbonic anhydrase 5B (CA5B) and the bicarbonate transporter SLC4A4 were markedly upregulated, whereas cytosolic carbonic anhydrase 2 (CA2) was downregulated (Fig. 5B). In the serine-one-carbon-folate (SOCF) pathway, key enzymes including SHMT1, SHMT2, and MTHFD1 were significantly upregulated in A549-ClpP cells (Fig. 5C). In addition, UPP1 and PGM2, which participate in uridine metabolism, were increased, whereas GLS, the rate-limiting enzyme in glutaminolysis, was downregulated (Fig. 5D and 5E). To determine whether these expression patterns were influenced by hypoxia, we analyzed gene expression under 1% O_2. CA5B, SHMT2, MTHFD1, and MTHFD2 remained upregulated under hypoxic conditions, while SLC4A4, despite being elevated under normoxia, was reduced under hypoxia (Fig. 5F-H). Notably, CA5B, SHMT2, and MTHFD1 were consistently elevated under both normoxic and hypoxic conditions, suggesting that activation of these pathways is a stable feature of the ClpP-associated metabolic phenotype. The increase in MTHFD1 expression was further confirmed at the protein level by western blotting. PHGDH, the rate-limiting enzyme in de novo serine biosynthesis, was also upregulated. Consistent with these findings, pharmacological activation of ClpP with ONC201 increased PHGDH and MTHFD1 protein expression in A549-EGFP cells (Fig. 5I). Collectively, these findings indicate that elevated ClpP expression is associated with coordinated remodelling of bicarbonate homeostasis, serine-one-carbon-folate metabolism, and uridine metabolism. These metabolic adaptations may contribute to cellular survival and persistence in acidic and hypoxic microenvironments.

Discussion

In this study, we demonstrate that ClpP expression in cancer cells is dynamically regulated in response to metabolic and environmental stress. While ClpP is well recognized for its role in mitochondrial proteostasis and oxidative phosphorylation, our findings reveal a previously unappreciated role for ClpP involving in adaption of cancer cells to nutrient limitation, extracellular acidification, and hypoxia. Specifically, we show that ClpP expression is bidirectionally regulated depending on the stress conditions encountered by the cells, and that increased ClpP expression is associated with metabolic remodeling that supports cellular fitness under adverse microenvironmental conditions. The principal finding of this study is that elevated ClpP is associated with metabolic adaptation and survival in response to nutrient limitation, extracellular acidification, and hypoxia. These findings expand the established role of ClpP beyond mitochondrial proteostasis and identify ClpP as a potential mediator of cancer cell metabolic plasticity in the stressed tumor microenvironment.

Although the primary focus of this study was the functional consequence of elevated ClpP expression, our data also reveal that ClpP is dynamically regulated by environmental and therapeutic stress. Metabolic stress induced by 2-DG and LY294002, and genotoxic stress induced by cisplatin elevated ClpP expression, whereas metformin, ONC201 and hypoxia down-regulated ClpP expression. Although these agents impose distinct forms of metabolic stress, existing evidence indicates that 2-DG [25, 26] and LY294002 [27, 28] restrict glucose utilization, while cisplatin has been reported to reduce glucose uptake in cisplatin-sensitive cancer cells [29, 30], while metformin and hypoxia generally enhance glucose consumption via increased glycolysis [21–23, 31]. The observed inverse relationship between ClpP expression and glucose utilization is further supported by findings in ClpP knockout mouse models, which exhibit increased glucose homeostasis [20, 32]. These findings suggest that ClpP forms part of a broader mitochondrial stress-adaptation program. A central finding of this study is the apparent link between ClpP expression and cellular acid-base homeostasis. Although ClpP-overexpressing cells accumulated extracellular lactate, they displayed markedly reduced medium acidification and survived substantially longer under prolonged culture conditions than control cells. Despite comparable lactate levels between control and ClpP-overexpressing A549 cells, the extracellular pH was significantly altered, suggesting the activation of buffering mechanisms capable of mitigating the detrimental effects of prolonged metabolic acid generation. In support of this idea, the mitochondrial CA5B was consistently among the most strongly induced genes in ClpP-overexpressing cells under both normoxic and hypoxic conditions. CA5B, unlike its liver-specific isoform CA5A, is broadly expressed but remains relatively understudied [33–35]. However, existing evidence shows that CA5B plays a critical role in ammonia detoxification and glucose metabolism and that overexpression of CA5B contributes to acid-base homeostasis and resistance to acidic microenvironment and hypoxia [36–40]. Altered expression of the bicarbonate transporter SLC4A4[41] further suggests coordinated remodeling of bicarbonate metabolism. Because bicarbonate represents the principal buffering system in the culture conditions used here, enhanced mitochondrial bicarbonate production may contribute to the preservation of intracellular pH homeostasis and the improved survival phenotype observed in ClpP-overexpressing cells. Although it remains unclear whether CA5B is a direct substrate of ClpP or is regulated indirectly through mitochondrial remodeling, our findings raise the possibility that ClpP contributes to adaptation to hostile microenvironments not only through metabolic rewiring but also through maintenance of acid-base balance. This potential ClpP–CA5B axis may represent a previously unrecognized connection between mitochondrial proteostasis and metabolic adaptation in cancer cells.

In addition to the apparent association with acid-base adaptation, ClpP overexpression was accompanied by extensive remodeling biosynthetic and nutrient-utilization pathways. Consistent with previous studies of ClpP [4, 10, 11, 20], elevated ClpP reduced electron transport chain (ETC) activity and decreased the NAD+/NADH ratio, indicating impaired oxidative metabolism. Despite these changes, intracellular ATP levels remained largely unchanged, suggesting engagement of compensatory metabolic programs [42].

Among the most prominent metabolic adaptations was the upregulation of enzymes involved in the SOCF metabolism, including SHMT1, SHMT2 and MTHFD1. This pathway plays a central role in

nucleotide synthesis, redox balance, and stress adaptation in cancer cells [43, 44]. The induction of these enzymes under both normoxic and hypoxic conditions suggests that increased SOCF metabolism is a consistent feature of the ClpP-associated phenotype. Increased expression of MTHFD1 and PHGDH at the protein level, together with their induction following ONC201 treatment, further supports a link between ClpP activity and metabolic pathways involved in biosynthesis and cellular maintenance.

Enhanced expression of UPP1 and PGM2 further suggests altered nucleotide salvage and uridine utilization in ClpP-overexpressing cells. Previous studies have shown that uridine metabolism can support glycolytic carbon utilization under nutrient-limited conditions [45]. Ribose-1-phosphate from uridine catabolism bypasses hexokinase to enter glycolysis, which probably explains the slightly increased sensitivity to 2-DG observed in ClpP overexpressing cells with impaired ETC function. Although the functional significance of these changes remains to be determined, the coordinated regulation of one-carbon and uridine metabolism is consistent with an adaptive response aimed at maintaining biosynthetic capacity under conditions of mitochondrial dysfunction.

From a therapeutic perspective, our findings suggest that the metabolic state of cancer cells may influence responses to ClpP-targeting therapies. Previous studies have reported enhanced activity of ClpP agonists when combined with cisplatin or glycolytic inhibition with 2-DG [46, 47], whereas hypoxia reduces sensitivity to ONC212, a second generation of ONC201[47]. Consistent with these observations, we found that cisplatin and 2-DG increased ClpP expression, whereas hypoxia reduced it. Although the underlying mechanisms remain unclear, these findings raise the possibility that stress-dependent regulation of ClpP contributes to therapeutic responsiveness and highlights the importance of considering metabolic context when evaluating ClpP-directed strategies.

In conclusion, our findings identify ClpP as a stress-responsive regulator associated with metabolic adaptation in cancer cells. Elevated ClpP expression enhances survival under nutrient deprivation and hypoxic conditions and is accompanied by coordinated changes in bicarbonate metabolism, serine-one-carbon metabolism, and uridine utilization. Although the mechanistic contribution of these pathways requires further investigation, the observed metabolic alterations provide a framework for understanding how elevated ClpP may support cellular fitness under adverse microenvironmental conditions. These findings expand the role of ClpP beyond mitochondrial proteostasis and highlight its potential importance in the metabolic adaptation of cancer cells.

Methods

Reagents, antibodies and kits

Metformin (Sigma, cat#PHR1084); 2-Deoxy-D-glucose (Sigma, cat# D8375); Cisplatin (Sigma, cat#PHR1624-200MG); LY294002 (Sigma, Cat#L9908-1MG); ONC201 (Sigma, SML1068). DMEM (ThermoFisher, cat# 31966047); Primary antibodies for western blot including: ClpP (Abcam; ab124822); SDHA (Abcam; ab14715); COXI (Abcam; ab14705); PHGDH (Abcam; ab240744); MTHFD1 (Abcam;

ab70203); β-actin (Sigma; A5441), and secondary antibodies: rabbit anti-mouse IgG (Dako P0260) and donkey anti-rabbit IgG (Santa Cruz; SC2313). For immunofluoressence: ClpP antibody (Thermo Fisher Scientific, cat. no. PA5-79051) and Alexa Fluor 488 goat anti-rabbit secondary antibody (MedChemExpress, cat. no. HY-P8002) as secondary antibody. Cell proliferation was determined with Cell Proliferation Kit II (XTT) kit (Sigma, cat#11465015001)

Cell lines

The human cell lines 143B, A549, and HepG2 were obtained from the American Type Culture Collection (ATCC). Primary lung fibroblasts were generated in our laboratory. All cells were cultured in Dulbecco's Modified Eagle's Medium (DMEM) supplemented with 10% fetal bovine serum (FBS) and 1× penicillin–streptomycin (Thermo Fisher Scientific, cat. no. 15140122). Cells were maintained at 37°C in a humidified incubator with 5% CO_2. For hypoxic growth condition, the cels were cultured in a humidified incubator with 1% O_2 level.

Establishment of stable cell lines overexpressing human ClpP

Human CLPP was cloned into pcDNA3.1-C-eGFP vector to generate a ClpP–EGFP fusion protein. Because the mitochondrial targeting sequence of ClpP is located at its N-terminal [3], EGFP was fused to the C- terminal of ClpP. Cell lines stably expressing ClpP–EGFP or EGFP were maintained in DMEM supplemented with 10% FBS and 1× penicillin–streptomycin in the presence of 200 μg/mL G418 (Sigma, cat. no. G8168).

Compound Treatments in Different Cancer Cell Lines Under Normoxia and Hypoxia

For compound treatment experiments, cells were seeded in 60-mm dishes. After 24 h, cells were treated with metformin, ONC201, cisplatin, 2-DG, or LY294002 under normoxic or hypoxic conditions. The specific cell types and compound concentrations are provided in the corresponding figures. After 2 days of treatment, cells were directly lysed in RIPA buffer (150 mM sodium chloride, 1.0% NP-40, 0.5% sodium deoxycholate, 0.1% sodium dodecyl sulfate, and 50 mM Tris, pH 8.0)

Western blot, Immunofluorescence, and Mitotracker staining

ClpP-EGFP expression was confirmed by Western blotting and immunofluorescence. For Western blot analysis, proteins were separated by SDS-PAGE, transferred to PVDF membranes, and analyzed using antibodies against ClpP and the indicated proteins. Signals were detected by enhanced chemiluminescence. For immunofluorescence, cells were fixed, permeabilized, stained with anti-ClpP antibody and fluorescent secondary antibody, counterstained with DAPI. Mitochondrial localization of

ClpP-EGFP was assessed by mitochondrial staining with MitoTracker® Red CMXRos (Thermo Fisher, M7512). Images were acquired using a ZEISS Observer 2.1 microscope.

Determination of IC50 of ONC201 in 143B Cell Lines

The 143B-ClpP1 and 143B-EGFP cell lines were used for IC50 determination. Briefly, 2,000 cells in 100 µL of DMEM were seeded in triplicate into 96-well plates. After 24 h, cells were treated with a 1:4 serial dilution of ONC201, with the highest concentration of ONC201 set at100 µM. Following 48 h of drug exposure, cell proliferation was accessed using XTT assay. The experiment was performed three times independently. IC50 values were calculated using GraphPad Prism (San Diego, USA).

Assessment of mitochondrial CI, CII, CIII and CIV activity in ClpP-EGFP overexpressing and EGFP-overexpressing 143B cells

Mitochondria were isolated from cells using the Mitochondrial Isolation Kit (Sigma; CatMITOISO2). Activities of mitochondrial complexes I–IV were assessed as described [48]. Briefly, complex I activity was measured using NADH as the electron donor and decylubiquinone as the intermediate electron carrier to reduce the colorimetric dye 2,6-dichloroindophenol (DCIP). Complex II activity was determined using succinate as substrate to reduce decylubiquinone and subsequently DCIP. Complex III activity was quantified by monitoring antimycin A and myxothiazol–sensitive reduction of cytochrome c using decylubiquinol as the electron donor. Complex IV activity was measured spectrophotometrically by monitoring cyanide-sensitive oxidation of reduced cytochrome c. All enzymatic assays were performed at 37°C.

Extraction of Polar Metabolites and Proteins from ClpP-EGFP overexpressing and EGFP overexpressing 143B Cells

A total of 2 × 10^5 143B- EGFP or 143B-ClpP1cells were seeded in 60-mm dishes and harvested three days later at confluence. Polar metabolites and total protein were extracted using a methanol–chloroform–water partitioning method. Briefly, cells were washed with ice-cold PBS, rapidly quenched with 80% methanol, scraped on ice, sonicated for 12 s, and sequentially mixed with chloroform and water to induce phase separation (4:3:2 v/v mixture of MeOH, $CHCl_3$ and H_2O). After centrifugation (18,000 g, 3 min, 0–4°C), the upper aqueous phase was collected, re-centrifuged, vacuum dried, and stored at − 80°C. The protein fraction was recovered from the interphase by addition of excess methanol and pelleting by centrifugation, dissolved in 2% SDS, sonicated, and quantified using a Bradford reagent containing 2.5 mg/ml α-cyclodextrin [49]. The polar metabolite fraction was used for ATP and NADH/NAD^+ measurements, and protein concentrations were used for normalization.

Enzymatic assays for ATP and NAD(H)

ATP levels and NAD(H) were quantified using published protocols [50, 51], respectively.

Measurement of the lactate concentrations in cell culture supernatants

Lactate concentrations in cell culture supernatants were quantified using a lactate assay kit (Sigma, MAK329). Briefly, 2 × 10^4 ClpP-EGFP–expressing A549 cells and their corresponding control cells, or 5 × 10^3 ClpP-EGFP–expressing 143B cells and their controls, were seeded in 24-well plates in 1 mL complete DMEM. Culture supernatants were collected on days 3, 6, and 10 for lactate measurement following the instruction of the kit. In parallel, cell numbers were determined using a Bürker chamber to assess cell proliferation, and cell pellets were harvested and stored at − 80°C for subsequent RNA isolation.

Gene expression determined with real-time PCR

Cellular total RNA was purified with RNeasy Mini Kit (Qiagen: 74106) and cDNA was synthesized with High-Capacity cDNA Reverse Transcription Kit (ThermoFisher Scientific: 4368814). Gene expression levels were analyzed with KAPA SYBR Fast Universal Kit (Sigma: KK4602). The human housekeeping gene 18s rRNA was used as a loading control. The primer sequences were listed in supplementary table 2.

Statistics

Statistical differences were tested by one-way ANOVA or Student *t* Test. $P < 0.05$ were considered statistically significant.

Abbreviations

2-DG
2-deoxyglucose
ATCC
American Type Culture Collection
ClpP
Caseinolytic peptidase P
OXPHOS
Oxidative Phosphorylation
ETC
Electron Transport Chain
CI
Complex I
CII
Complex II
CIII
Complex III
CIV

Complex IV
CA5B
Carbonic Anhydrase 5B

Declarations

Consent for publication

Not applicable.

Conflict of Interest statement

The authors declare that they have no competing interests.

Funding

The study was funded by The Swedish Cancer Society (grants 20 0681 ReVS 01 H, 20 0730 PjVSF 01 H).

Author Contribution

SC and XZ designed the project and performed most of the experiments. JP carried out nucleotide quantifications and contributed to the OXPHOS activity assays. FF and WW assisted with project design. XZ wrote the manuscript, with contributions from SC and JP.

References

1. Armenise D, Baldelli OM, Liturri A, Cavallaro G, Fortuna CG, Ferorelli S, Miciaccia M, Perrone MG, Scilimati A. Mitochondrial Protease ClpP: Cancer Marker and Drug Target. Pharmaceuticals (Basel) 2025, 18(10).
2. Currie SQW, Goncalves MM, Schimmer AD, Vahidi S. Molecular mechanisms of mitochondrial AAA+ proteases. J Biol Chem. 2026;302(3):111264.
3. Nouri K, Feng Y, Schimmer AD. Mitochondrial ClpP serine protease-biological function and emerging target for cancer therapy. Cell Death Dis. 2020;11(10):841.
4. Cole A, Wang ZZ, Coyaud E, Voisin V, Gronda M, Jitkova Y, Mattson R, Hurren R, Babovic S, Maclean N, et al. Inhibition of the Mitochondrial Protease ClpP as a Therapeutic Strategy for Human Acute Myeloid Leukemia. Cancer Cell. 2015;27(6):864–76.
5. Luo J, Zeng B, Tao C, Lu M, Ren G. ClpP regulates breast cancer cell proliferation, invasion and apoptosis by modulating the Src/PI3K/Akt signaling pathway. PeerJ. 2020;8:e8754.

6. Seo JH, Rivadeneira DB, Caino MC, Chae YC, Speicher DW, Tang HY, Vaira V, Bosari S, Palleschi A, Rampini P, et al. The Mitochondrial Unfoldase-Peptidase Complex ClpXP Controls Bioenergetics Stress and Metastasis. PLoS Biol. 2016;14(7):e1002507.
7. Perini T, Zordan P, Del Pizzo R, Resnati M, Viviani L, Stefanoni D, Cassina L, Orfanelli U, Trudu M, Oliva L, et al. The mitochondrial protease ClpP is a metabolic vulnerability and an immunogenic trigger against multiple myeloma. Blood. 2025;146(11):1286–99.
8. Cormio A, Sanguedolce F, Pesce V, Musicco C. Mitochondrial Caseinolytic Protease P: A Possible Novel Prognostic Marker and Therapeutic Target in Cancer. Int J Mol Sci 2021, 22(12).
9. Lee YG, Kim HW, Nam Y, Shin KJ, Lee YJ, Park DH, Rhee HW, Seo JK, Chae YC. LONP1 and ClpP cooperatively regulate mitochondrial proteostasis for cancer cell survival. Oncogenesis. 2021;10(2):18.
10. Ishizawa J, Zarabi SF, Davis RE, Halgas O, Nii T, Jitkova Y, Zhao R, St-Germain J, Heese LE, Egan G, et al. Mitochondrial ClpP-Mediated Proteolysis Induces Selective Cancer Cell Lethality. Cancer Cell. 2019;35(5):721–e737729.
11. Lim B, Peterson CB, Davis A, Cho E, Pearson T, Liu H, Hwang M, Ueno NT, Lee J. ONC201 and an MEK Inhibitor Trametinib Synergistically Inhibit the Growth of Triple-Negative Breast Cancer Cells. Biomedicines 2021, 9(10).
12. Arrillaga-Romany I, Gardner SL, Odia Y, Aguilera D, Allen JE, Batchelor T, Butowski N, Chen C, Cloughesy T, Cluster A, et al. ONC201 (Dordaviprone) in Recurrent H3 K27M-Mutant Diffuse Midline Glioma. J Clin Oncol. 2024;42(13):1542–52.
13. Atkins SLP, Greer YE, Jenkins S, Gatti-Mays ME, Houston N, Lee S, Lee MJ, Rastogi S, Sato N, Burks C, et al. A Single-Arm, Open-Label Phase II Study of ONC201 in Recurrent/Refractory Metastatic Breast Cancer and Advanced Endometrial Carcinoma. Oncologist. 2023;28(10):919–e972.
14. Clymer J, Kieran MW. The Integration of Biology Into the Treatment of Diffuse Intrinsic Pontine Glioma: A Review of the North American Clinical Trial Perspective. Front Oncol 2018, 8.
15. Khasraw M, Dun MD, Arrillaga-Romany I, Verhaak RGW, Bouffet E, Hansford JR, Singh K, Mueller S, Koschmann C, Wen PY. Dordaviprone for Diffuse Midline Glioma: A Landmark Approval or a Premature. Step? Neuro Oncol; 2026.
16. Cao J, Cao F, Wang C, Jiao Z, You Y, Wang X, Zhao W. ONC206 targeting ClpP induces mitochondrial dysfunction and protective autophagy in hepatocellular carcinoma cells. Neoplasia. 2024;55:101015.
17. Ishizawa J, Zarabi SF, Davis RE, Halgas O, Nii T, Jitkova Y, Zhao R, St-Germain J, Heese LE, Egan G, et al. Mitochondrial ClpP-Mediated Proteolysis Induces Selective Cancer Cell Lethality. Cancer Cell. 2019;35(5):721–.
18. Lim B, Peterson CB, Davis A, Cho EL, Pearson T, Liu HY, Hwang M, Ueno NT, Lee JS. ONC201 and an MEK Inhibitor Trametinib Synergistically Inhibit the Growth of Triple-Negative Breast Cancer Cells. Biomedicines 2021, 9(10).

19. Wang SM, Dougan DA. The Direct Molecular Target for Imipridone ONC201 Is Finally Established. Cancer Cell. 2019;35(5):707–8.
20. Becker C, Kukat A, Szczepanowska K, Hermans S, Senft K, Brandscheid CP, Maiti P, Trifunovic A. CLPP deficiency protects against metabolic syndrome but hinders adaptive thermogenesis. EMBO Rep 2018, 19(5).
21. Andrzejewski S, Gravel SP, Pollak M, St-Pierre J. Metformin directly acts on mitochondria to alter cellular bioenergetics. Cancer Metab 2014, 2.
22. Singh SV, Chaube B, Mayengbam SS, Singh A, Malvi P, Mohammad N, Deb A, Bhat MK. Metformin induced lactic acidosis impaired response of cancer cells towards paclitaxel and doxorubicin: Role of monocarboxylate transporter. Bba-Mol Basis Dis 2021, 1867(3).
23. Yang M, Darwish T, Larraufie P, Rimmington D, Cimino I, Goldspink DA, Jenkins B, Koulman A, Brighton CA, Ma M et al. Inhibition of mitochondrial function by metformin increases glucose uptake, glycolysis and GDF-15 release from intestinal cells. *Sci Rep-Uk* 2021, 11(1).
24. Wedam R, Greer YE, Wisniewski DJ, Weltz S, Kundu M, Voeller D, Lipkowitz S. Targeting Mitochondria with ClpP Agonists as a Novel Therapeutic Opportunity in Breast Cancer. Cancers 2023, 15(7).
25. Singh R, Gupta V, Kumar A, Singh K. 2-Deoxy-D-Glucose: A Novel Pharmacological Agent for Killing Hypoxic Tumor Cells, Oxygen Dependence-Lowering in Covid-19, and Other Pharmacological Activities. *Adv Pharmacol Pharm Sci* 2023, 2023:9993386.
26. Pajak B, Siwiak E, Soltyka M, Priebe A, Zielinski R, Fokt I, Ziemniak M, Jaskiewicz A, Borowski R, Domoradzki T et al. 2-Deoxy-d-Glucose and Its Analogs: From Diagnostic to Therapeutic Agents. Int J Mol Sci 2020, 21(1).
27. Lu J, Chen M, Gao SM, Yuan JG, Zhu Z, Zou XP. LY294002 inhibits the Warburg effect in gastric cancer cells by downregulating pyruvate kinase M2. Oncol Lett. 2018;15(4):4358–64.
28. Duarte A, Silveira GG, Soave DF, Costa JPO, Silva AR. The Role of the LY294002 - A Non-Selective Inhibitor of Phosphatidylinositol 3-Kinase (PI3K) Pathway- in Cell Survival and Proliferation in Cell Line SCC-25. Asian Pac J Cancer Prev. 2019;20(11):3377–83.
29. Egawa-Takata T, Endo H, Fujita M, Ueda Y, Miyatake T, Okuyama H, Yoshino K, Kamiura S, Enomoto T, Kimura T, et al. Early reduction of glucose uptake after cisplatin treatment is a marker of cisplatin sensitivity in ovarian cancer. Cancer Sci. 2010;101(10):2171–8.
30. Wang SJ, Xie J, Li JJ, Liu F, Wu XH, Wang ZL. Cisplatin suppresses the growth and proliferation of breast and cervical cancer cell lines by inhibiting integrin β5-mediated glycolysis. Am J Cancer Res. 2016;6(5):1108–.
31. Sureka N, Maheshwari R, Agravat A, Singhal S, Zaman S, Rishi B, Siraj F, Zaheer S, Misra A. Hypoxic microenvironment in cancer: role in metabolic reprogramming. Front Oncol. 2026;16:1771365.
32. Bhaskaran S, Pharaoh G, Ranjit R, Murphy A, Matsuzaki S, Nair BC, Forbes B, Gispert S, Auburger G, Humphries KM et al. Loss of mitochondrial protease ClpP protects mice from diet-induced obesity and insulin resistance. EMBO Rep 2018, 19(3).

33. Bernardino RL, Dias TR, Moreira BP, Cunha M, Barros A, Oliveira E, Sousa M, Alves MG, Oliveira PF. Carbonic anhydrases are involved in mitochondrial biogenesis and control the production of lactate by human Sertoli cells. FEBS J. 2019;286(7):1393–406.
34. Fujikawa-Adachi K, Nishimori I, Taguchi T, Onishi S. Human mitochondrial carbonic anhydrase VB. cDNA cloning, mRNA expression, subcellular localization, and mapping to chromosome x. J Biol Chem. 1999;274(30):21228–33.
35. Shah GN, Hewett-Emmett D, Grubb JH, Migas MC, Fleming RE, Waheed A, Sly WS. Mitochondrial carbonic anhydrase CA VB: differences in tissue distribution and pattern of evolution from those of CA VA suggest distinct physiological roles. Proc Natl Acad Sci U S A. 2000;97(4):1677–82.
36. Aventaggiato M, Arcangeli T, Vernucci E, Barreca F, Sansone L, Pellegrini L, Pontemezzo E, Valente S, Fioravanti R, Russo MA et al. Pharmacological Activation of SIRT3 Modulates the Response of Cancer Cells to Acidic pH. Pharmaceuticals (Basel) 2024, 17(6).
37. Huang R, Liu X, Li H, Zhou Y, Zhou PK. Integrated analysis of transcriptomic and metabolomic profiling reveal the p53 associated pathways underlying the response to ionizing radiation in HBE cells. Cell Biosci. 2020;10:56.
38. Pellegrini L, Pucci B, Villanova L, Marino ML, Marfe G, Sansone L, Vernucci E, Bellizzi D, Reali V, Fini M, et al. SIRT3 protects from hypoxia and staurosporine-mediated cell death by maintaining mitochondrial membrane potential and intracellular pH. Cell Death Differ. 2012;19(11):1815–25.
39. Postel R, Sonnenberg A. Carbonic anhydrase 5 regulates acid-base homeostasis in zebrafish. PLoS ONE. 2012;7(6):e39881.
40. Shah GN, Rubbelke TS, Hendin J, Nguyen H, Waheed A, Shoemaker JD, Sly WS. Targeted mutagenesis of mitochondrial carbonic anhydrases VA and VB implicates both enzymes in ammonia detoxification and glucose metabolism. P Natl Acad Sci USA. 2013;110(18):7423–8.
41. Cappellesso F, Orban MP, Shirgaonkar N, Berardi E, Serneels J, Neveu MA, Di Molfetta D, Piccapane F, Caroppo R, Debellis L, et al. Targeting the bicarbonate transporter SLC4A4 overcomes immunosuppression and immunotherapy resistance in pancreatic cancer. Nat Cancer. 2022;3(12):1464–83.
42. Bajzikova M, Kovarova J, Coelho AR, Boukalova S, Oh S, Rohlenova K, Svec D, Hubackova S, Endaya B, Judasova K, et al. Reactivation of Dihydroorotate Dehydrogenase-Driven Pyrimidine Biosynthesis Restores Tumor Growth of Respiration-Deficient Cancer Cells. Cell Metab. 2019;29(2):399–416. e310.
43. Ducker GS, Rabinowitz JD. One-Carbon Metabolism in Health and Disease. Cell Metabol. 2017;25(1):27–42.
44. Martínez-Reyes I, Chandel NS. Mitochondrial One-Carbon Metabolism Maintains Redox Balance during Hypoxia. Cancer Discov. 2014;4(12):1371–3.
45. Skinner OS, Blanco-Fernandez J, Goodman RP, Kawakami A, Shen H, Kemeny LV, Joesch-Cohen L, Rees MG, Roth JA, Fisher DE, et al. Salvage of ribose from uridine or RNA supports glycolysis in nutrient-limited conditions. Nat Metab. 2023;5(5):765–76.

46. Chuang HC, Tsai MH, Chuang JH, Hong YT, Chien CY, Chou MH. ONC201 enhances the cytotoxic effect of cisplatin through ATF3/ATF4/CHOP in head and neck squamous cell carcinoma cells. Oncogenesis 2025, 14(1).
47. Ferrarini I, Louie A, Zhou LL, El-Deiry WS. ONC212 is a Novel Mitocan Acting Synergistically with Glycolysis Inhibition in Pancreatic Cancer. Mol Cancer Ther. 2021;20(9):1572–83.
48. Purhonen J, Grigorjev V, Ekiert R, Aho N, Rajendran J, Pietras R, Truve K, Wikstrom M, Sharma V, Osyczka A, et al. A spontaneous mitonuclear epistasis converging on Rieske Fe-S protein exacerbates complex III deficiency in mice. Nat Commun. 2020;11(1):322.
49. Rabilloud T. Optimization of the cydex blue assay: A one-step colorimetric protein assay using cyclodextrins and compatible with detergents and reducers. PLoS ONE. 2018;13(4):e0195755.
50. Purhonen J, Grigorjev V, Ekiert R, Aho N, Rajendran J, Pietras R, Truvé K, Wikström M, Sharma V, Osyczka A et al. A spontaneous mitonuclear epistasis converging on Rieske Fe-S protein exacerbates complex III deficiency in mice. Nat Commun 2020, 11(1).
51. Purhonen J, Hofer A, Kallijärvi J. Quantification of all 12 canonical ribonucleotides by real-time fluorogenic in vitro transcription. Nucleic Acids Res 2024, 52(1).

Figures

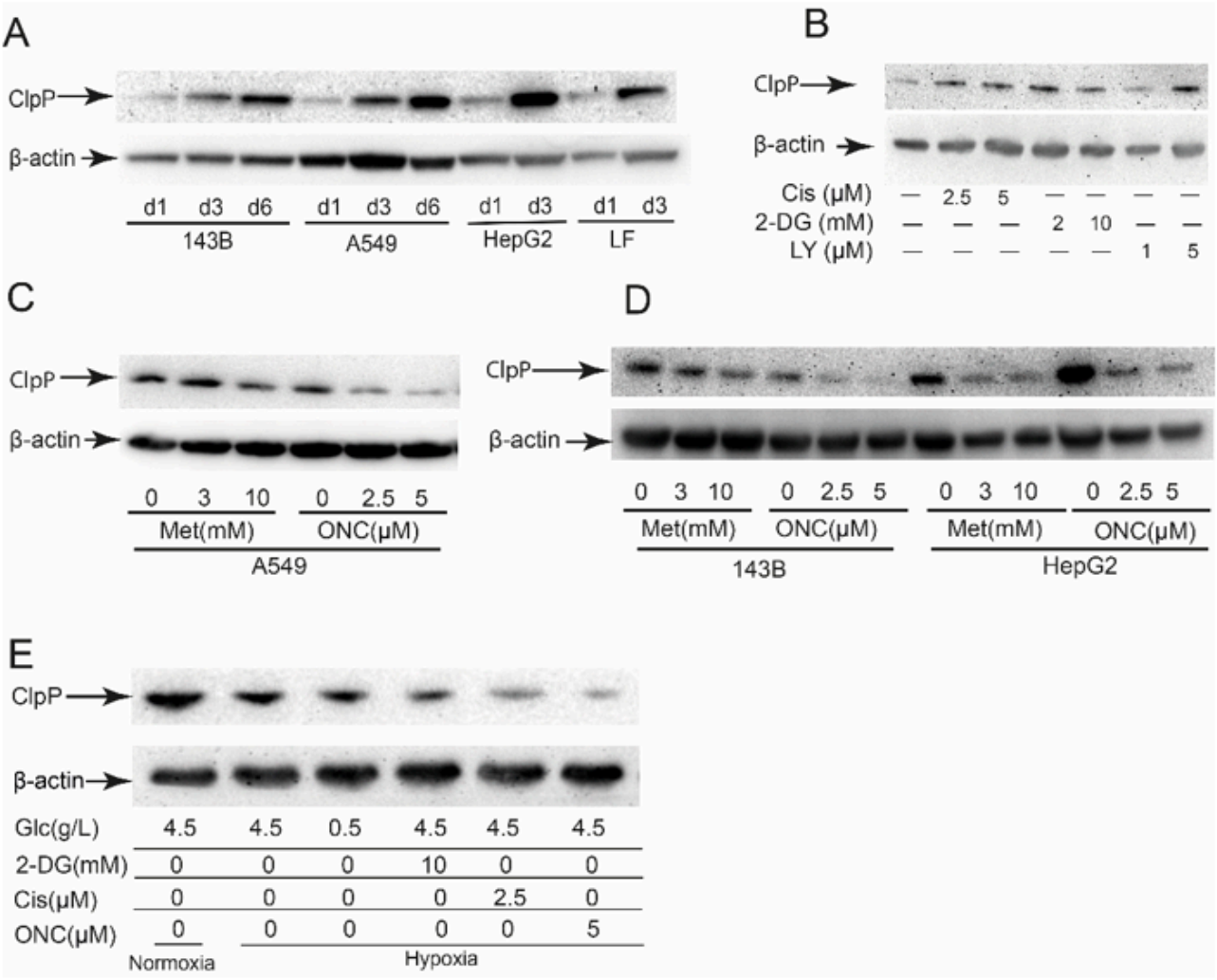


Figure 1

ClpP expression under different types of stresses. (A) ClpP expression levels under prolonged culture in different cell lines. (B) Enhanced ClpP expression induced by cisplatin, 2-DG, and LY294002. (C and D) Decreased ClpP expression by metformin and ONC201 in (C) A549 and in (D) 143B and HepG2 cells. Respectively. (E) Impact of hypoxia on ClpP Expression in 143B cells. Met: metformin; ONC: ONC201; Cis: cisplatin; Glc: glucose; LY: LY294002.

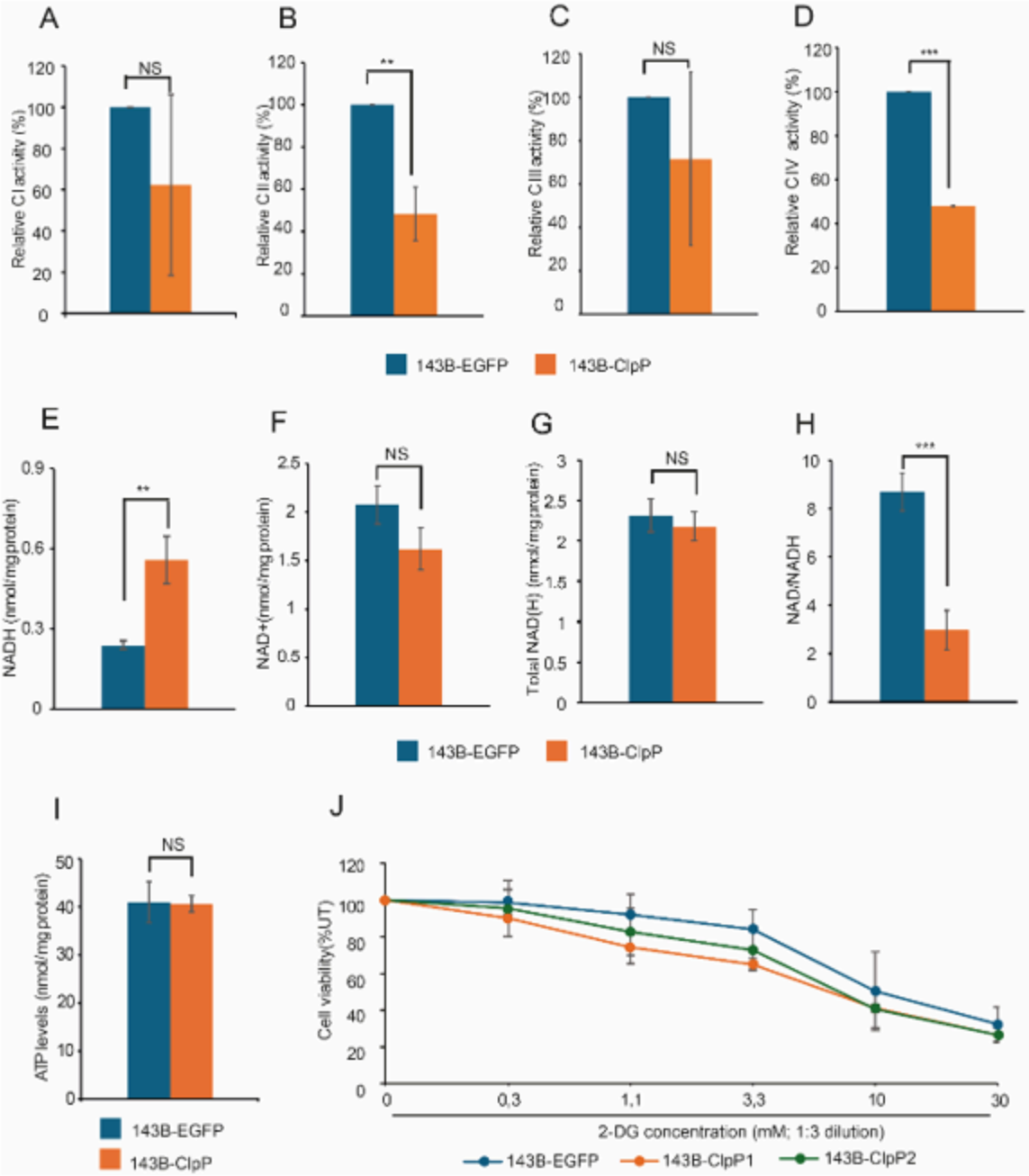


Figure 2

Effects of ClpP overexpression on celluar energy metabolism in 143B-ClpP cells. (A) mitochondrial complex I (CI) activity. (B) CII activity. (C) CIII activity. (D) CIV activity. (E) Cellular NADH level. (F) Cellular NAD^+ level. (G) Total NAD(H). (H) NAD^+/NADH ratio. (I) Cellular level of ATP. (J) Sensitivity to 2-DG treatment. 143B-ClpP1 and 143B-ClpP2 represent 2 different ClpP overexpression clones. All the experiments were repeated 3 times and data are represented as mean value ± SD. Statistical significance was assessed using the student's test. **:P<0.01; *** P<0.001.

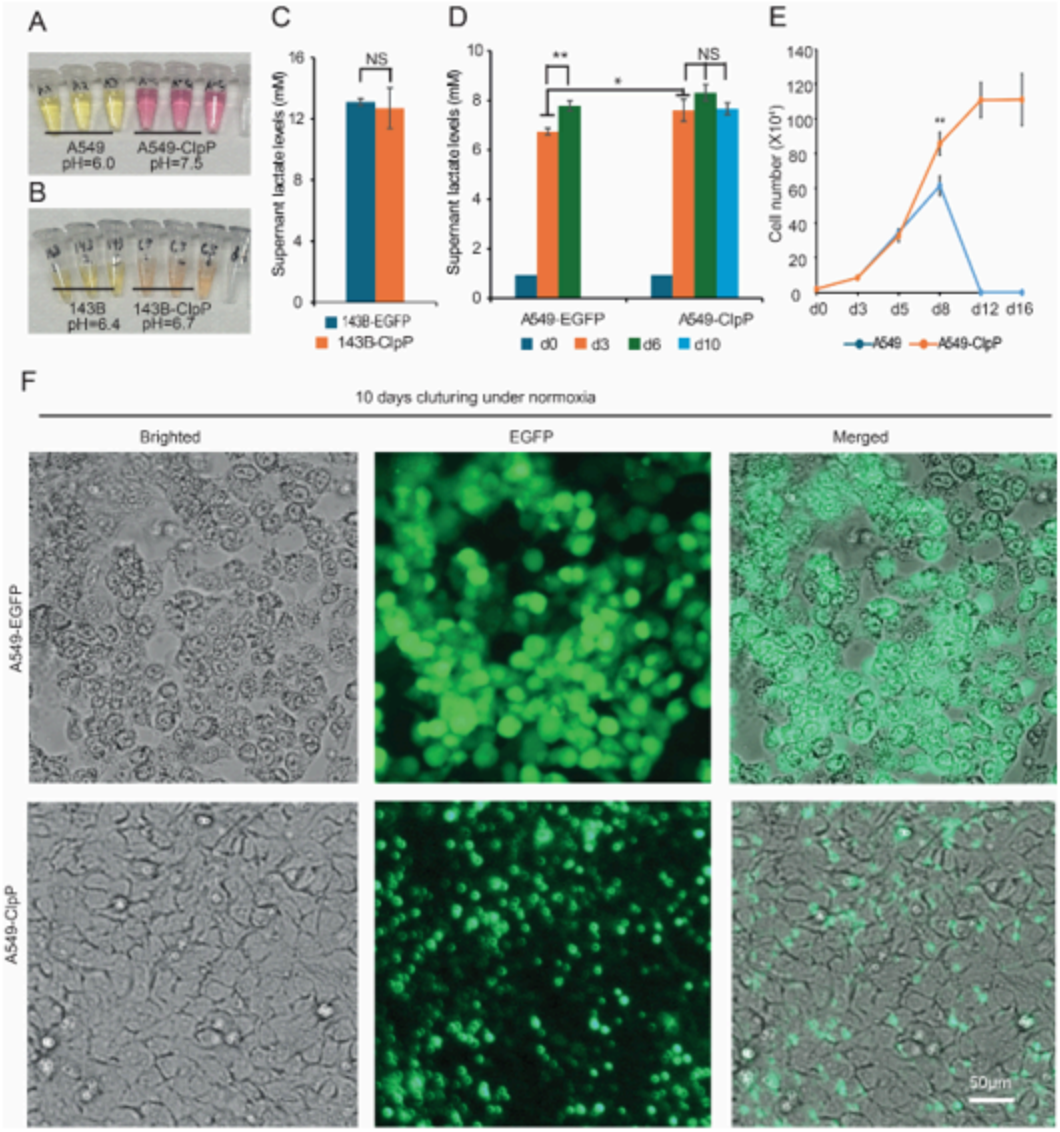


Figure 3

Cells overexpressing ClpP exhibit reduced extracellular acidification and enhanced survival during prolonged culture

(A, B) Representative images showing culture medium color changes in A549 (A) and 143B (B) cells after 4 days of culture. (C) Lactate concentrations in conditioned medium collected from 143B cell lines on 3 days of culture. (D) Lactate concentrations in conditioned medium collected from A549 cell lines at the indicated time points following seeding. (E) Growth curves of A549-ClpP and A549-EGFP cells cultured under normoxic conditions without medium replacement. Data are presented as mean cell number ± SD from triplicate wells of a 24-well plate. (F) Representative images of A549-ClpP and A549-EGFP cells after 10 days of culture without medium replacement. Data are presented as mean ± SD. Statistical significance was determined using a two-tailed Student's t-test or one-way ANOVA test. *: $P < 0.05$; **: $P < 0.01$.

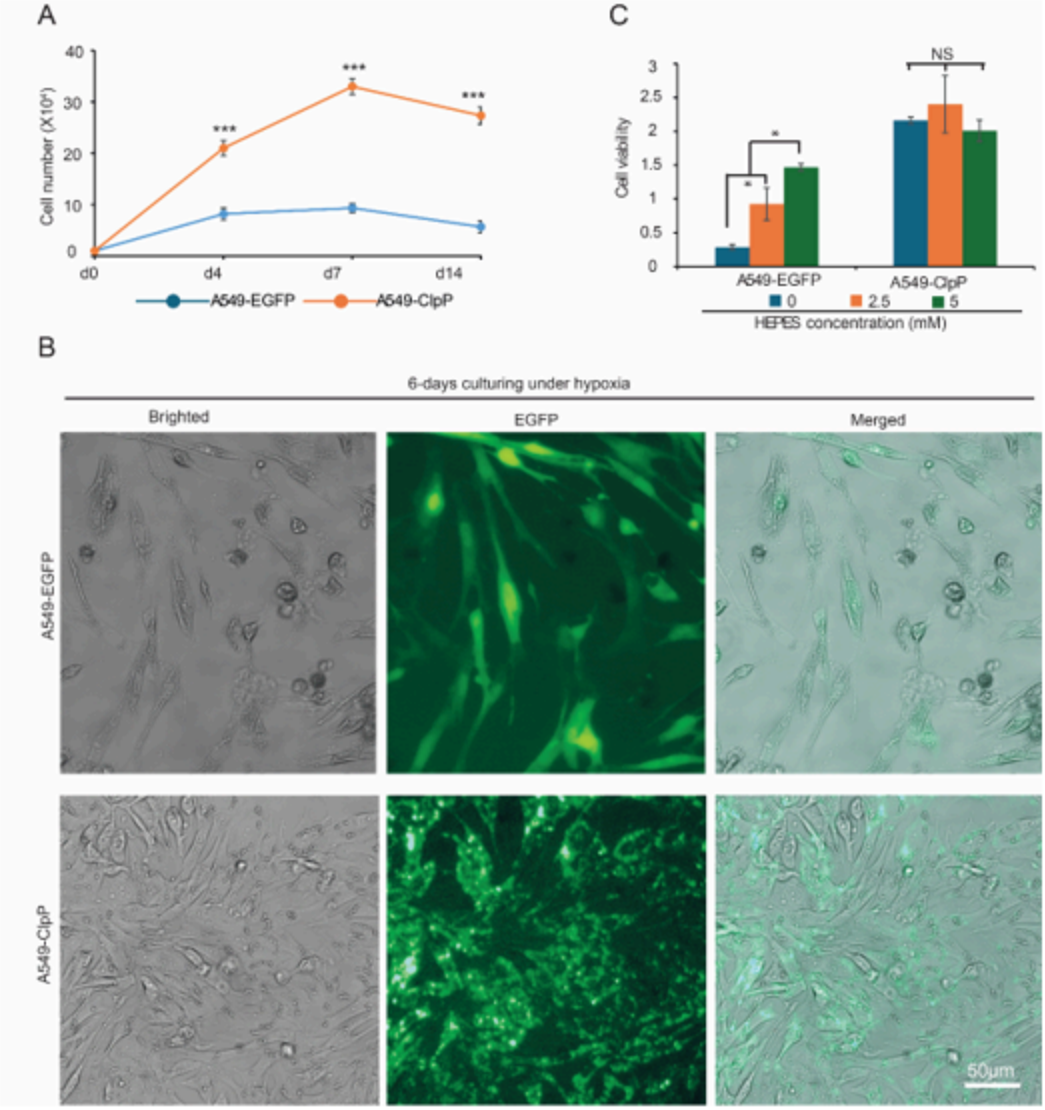


Figure 4

ClpP overexpression enhances cancer cell survival under hypoxic conditions

(A) Growth curves of A549-ClpP and A549-EGFP cells under hypoxic conditions (1% O_2) without medium replacement. Data are presented as mean cell number ± SD from triplicate wells of a 24-well plate. (B) Representative images of A549-ClpP and A549-EGFP cells cultured under hypoxic conditions. A549-EGFP cells underwent a pronounced morphological transition from a cobblestone-like epithelial phenotype to an elongated, spindle-shaped morphology. In contrast, A549-ClpP cells largely retained their epithelial morphology and reached confluency. (C) Effect of enhanced medium buffering on the viability of A549-ClpP and A549-EGFP cells cultured under normoxic conditions. Cells were cultured in medium supplemented with the indicated concentrations of HEPES. Data are represented as mean ± SD of three independent experiments. Statistical significance was determined by student t test or one-way ANOVA. *:P<0.05; *** P<0.001.

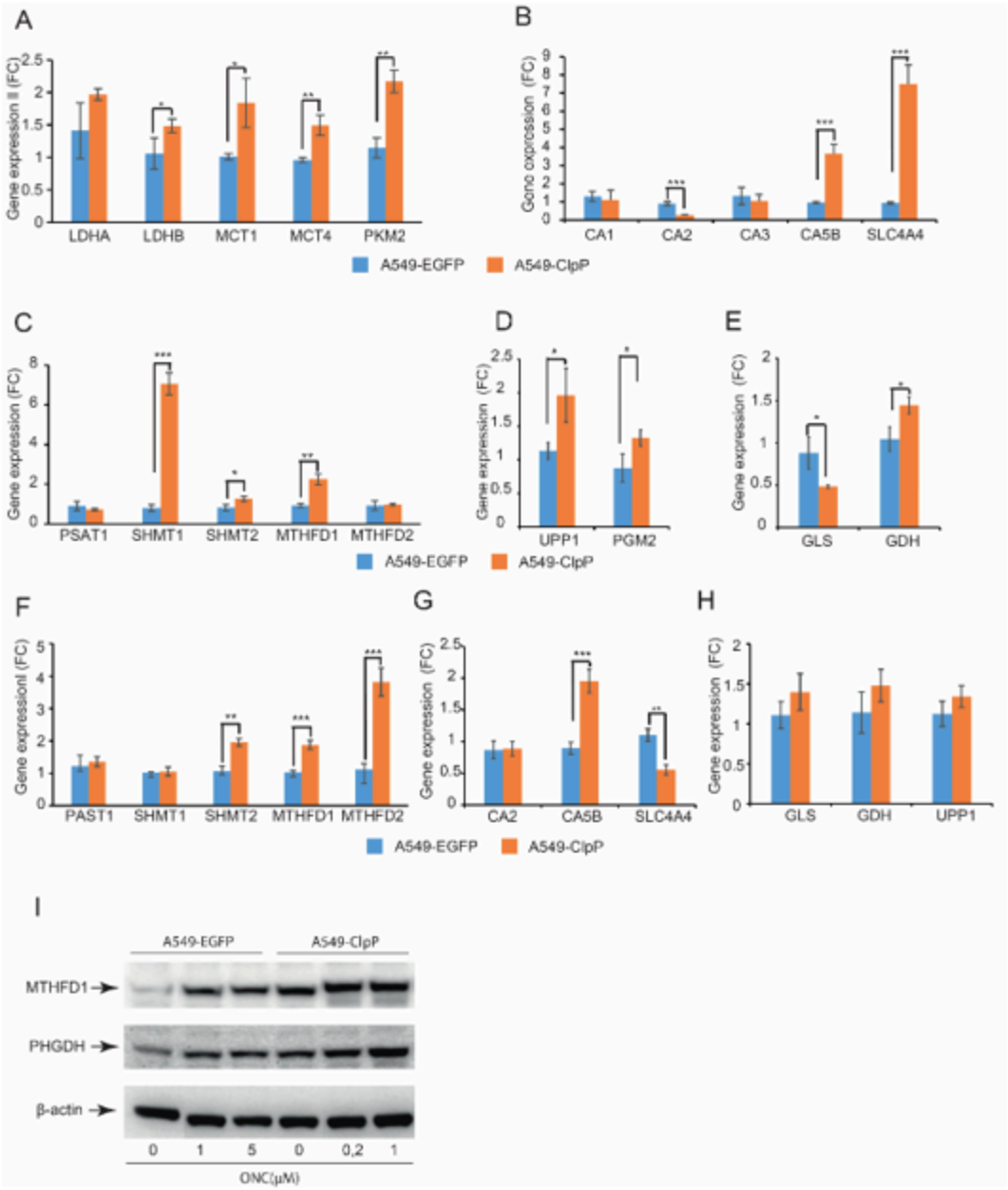


Figure 5

Effects of ClpP overexpression on the expression of genes involved in cell metabolism in A549 cells. (A-E) Genes involved in: (A) lactate metabolism; (B) bicarbonate metabolism; (C) serine-folate metabolism; (D) uridine and (E) glutamine metabolisms. (F-H) Under hypoxia, expression of genes in: (F) serine-folate metabolism; (G) bicarbonate metabolism and (H) uridine and glutamine metabolisms. (I) Western blot determining MTHFD1 and PHGDH protein levels. ONC: ONC201. The experiments for analyzing gene expression were repeated 3 times and data are represented as mean value of fold changes ± SD. Statistical significance was assessed using the student's test. * p<0,05; **:P<0.01; *** P<0.001.

Supplementary Files

This is a list of supplementary files associated with this preprint. Click to download.

- BetaactinforFigure1C.tif
- BetaactinforFigure1C.tif
- BetactinforFigure1A.tif
- BetaactinforFigure1D.tif
- ClpPforFigure1C.tif
- ClpPforFigure1D.tif
- BetaactinFigure1F.tif
- ClpPforFigure1A.tif
- BetaactinforFigure1B.tif
- ClpPforFigure1F.tif
- ClpPforFigure1B.tif
- Supplementaryinformation.docx
- supplementaryFigure2Cbetaactin.tif
- Figure5GPHGDHcopy.tif
- Figure5Gbetaactincopy.tif
- Figure5GPHGDH.tif
- supplementaryFigure2CClpPClpPEGFP.tif